THE JOURNAL OF BIOLOGICAL CHEMISTRY
Vol. 273, No. 31, Issue of July 31, pp. 19625–19633, 1998

*Printed in U.S.A.*

# Cellubrevin-targeted Fluorescence Uncovers Heterogeneity in the Recycling Endosomes*

(Received for publication, January 16, 1998, and in revised form, May 8, 1998)

**Ken Teter‡, Grischa Chandy, Beatriz Quiñones, Kristina Pereyra‡, Terry Machen, and Hsiao-Ping H. Moore§**

*From the Department of Molecular and Cell Biology, University of California, Berkeley, California 94720-3200*

**The pH and trafficking of recycling endosomes have previously been studied using transferrin. We have used another approach, one in which the vesicle transport protein cellubrevin was appended with a luminal IgG epitope to allow targeting of fluorescein-5′-isothiocyanate (FITC)-labeled anti-IgG F(ab) antibodies to the recycling endosomes in living cells. FITC-F(ab) was specifically internalized by COS cells transfected with cellubrevin-Ig, which at steady state accumulated in a pericentriolar region similar to rhodamine-transferrin. Confocal microscopic analysis showed that endosome labeling by these two markers was heterogeneous. This differential distribution was not induced by the IgG tag, since endogenous Cb and Tf were also partitioned into separate endosomal populations. We used fluorescence ratio imaging of internalized FITC-F(ab) to measure the pH of cellubrevin-enriched recycling endosomes ($pH_{Cb}$) and FITC-transferrin to measure the pH of transferrin-enriched recycling endosomes ($pH_{Tf}$). In COS cells, cellubrevin endosomes (mean $pH_{Cb}$ 6.1 ± 0.05; range, 5.2–6.6) were more acidic than transferrin endosomes (mean $pH_{Tf}$ 6.5 ± 0.05; range, 5.6–7.2). Similar results were obtained in Chinese hamster ovary cells. Treatment with the vacuolar $H^+$-ATPase inhibitor bafilomycin $A_1$ caused $pH_{Tf}$ to increase ($\Delta pH_{Tf}$ = 1.2 pH units) to a greater extent than $pH_{Cb}$ ($\Delta pH_{Cb}$ = 0.5 pH units). Furthermore, inhibition of the $Na^+/K^+$-ATPase by ouabain or acetylstrophanthidin caused $pH_{Tf}$ to decrease by 0.6 pH units but had no effect on $pH_{Cb}$. Based on the combination of these morphological and functional data, we suggest that the recycling endosomes are heterogeneous in their biochemical compositions, ion transport properties, and pH values.**

The cycling of molecules through the endocytic pathway has been extensively studied by monitoring the trafficking of the transferrin-transferrin receptor (Tf·TfR)[1] complex (reviewed in Refs. 1 and 2). Surface-bound Tf is concentrated into coated pits and internalized in endocytic vesicles, which rapidly fuse with sorting endosomes, the population of early endosomes scattered throughout the cell periphery (3–7). The low luminal pH (~6.0) of the sorting endosomes promotes dissociation of $Fe^{3+}$ from the bound Tf (8, 9), and the Tf·TfR complex is then segregated into tubular extensions that exclude the now soluble $Fe^{3+}$ (10). These tubular elements bud from the sorting endosomes and return the complex to the cell surface, where TfR can reload with $Fe^{3+}$-Tf to repeat the cycle. On the recycling pathway, most of the Tf·TfR complex clusters at a distinct perinuclear location in close apposition to the microtubule organizing center. These perinuclear recycling endosomes are distinguished from sorting endosomes by their distinct intracellular location and by the lack of cargo destined for late endosomes and lysosomes (3, 4, 6, 11).

Despite the consistent picture emerging from experiments investigating Tf and TfR, recent biochemical and immunomicroscopic observations have suggested that the endosomal pathway is more complex than was originally perceived. Several membrane proteins that cycle through the endosomal system have overlapping but distinct distributions, suggesting that they may not always follow the same path (for example, see Refs. 12–14). Many components of the vesicular traffic machinery are also heterogeneously distributed among endosomes. The low molecular weight GTPases Rab4 and Rab11 are both associated with subpopulations of perinuclear recycling endosomes (15, 16). Cellubrevin (Cb), a v-SNARE protein involved in TfR recycling, is associated with many peripheral vesicles that do not contain TfR (17, 18). Likewise, in neuroendocrine cells Cb is targeted to neurites that exclude the TfR (19).

At present, the physiological properties and functional roles of the putative endosome subpopulations are not known. Endosomal pH measurements using dye-labeled Tf in conjunction with either cytofluorometry or cellular imaging have shown that peripheral sorting endosomes have a pH in the range of 5.9–6.4 (20–24), while the perinuclear recycling endosomes have a slightly higher pH of 6.4 (4, 22–24). As a first step to determine the physiological heterogeneity of recycling endosomes, we have devised a "targeted fluorescence" approach to observe the distribution and pH of Cb-containing recycling vesicles. Cb was chosen because it is a constituent of the recycling endosomes, but, as discussed above, previous experiments suggested that it does not always co-distribute with Tf. Therefore, measurements made with this marker could conceivably

* This work was supported by National Institutes of Health (NIH) Grants GM35239 (to H. P. M.) and DK95006 (to T. M.) and grants from CRCC (to H. P. M.) and Cystic Fibrosis Research, Inc. (to T. M. and H. P. M.). The costs of publication of this article were defrayed in part by the payment of page charges. This article must therefore be hereby marked "*advertisement*" in accordance with 18 U.S.C. Section 1734 solely to indicate this fact.

‡ K. Teter and K. Pereyra were supported by an NIH training grant to the Department of Molecular and Cell Biology.

§ To whom correspondence should be addressed: Dept. of Molecular and Cell Biology, 142 Life Sciences Addition #3200, University of California, Berkeley, CA 94720-3200. Tel.: 510-643-6528; Fax: 510-643-8708; E-mail: hpmoore@uclink4.berkeley.edu.

[1] The abbreviations used are: Tf, transferrin; TfR, transferrin receptor; hIgG, human immunoglobulin G; Cb, cellubrevin; Cb-Ig, cellubrevin-immunoglobulin fusion protein; BCECF-AM, 2′,7′-bis-(2-carboxyethyl)-5 (and -6)-carboxyfluorescein acetoxymethylester; $pH_{Cb}$, pH of Cb-Ig-containing recycling endosomes; $pH_{Tf}$, pH of Tf-containing recycling endosomes; $pH_c$, cytosolic pH; FITC, fluorescein-5′-isothiocyanate; Rh, rhodamine; TGN, *trans*-Golgi network; ER, endoplasmic reticulum; CHO, Chinese hamster ovary; DABCO, 1,4-diazabicyclo[2.2.2]octane; GalT, galactosyltransferase; UDPGT, UDP-glucuronyltransferase; PBS, phosphate-buffered saline; BSA, bovine serum albumin; DMEM, Dulbecco's modified Eagle's medium.

reveal physiological differences within the recycling endosomes that may have been overlooked by the Tf-based work. A fusion protein of Cb and the human IgG constant region was created to allow targeting of pH-sensitive dyes to Cb-containing recycling endosomes. We stably transfected COS-7 cells with the Cb-Ig construct and performed a series of experiments to determine (i) the cellular distribution of FITC-labeled anti-IgG F(ab) fragment added to the extracellular media of live cells, (ii) the pH of the Cb-containing recycling endosomes, and (iii) the roles of the $H^+$-ATPase and $Na^+/K^+$-ATPase in governing Cb-containing recycling endosome pH. These results were compared with data obtained from similar experiments using Tf as the recycling endosome marker. Our results indicated that there are subpopulations of perinuclear recycling endosomes that can be visualized by confocal microscopy and are further distinguished by differences in pH and responses to ouabain and bafilomycin $A_1$. The potential roles of the recycling endosome subpopulations are discussed.

## EXPERIMENTAL PROCEDURES

*Materials*—All salts, bafilomycin $A_1$, nocodazole, ouabain, chloroquine, paraformaldehyde, hygromycin B, acetylstrophanthidin, fetal calf serum, DEAE-dextran and DABCO were purchased from Sigma. Glycerol, methanol, and acetic acid were from Fisher, and restriction enzymes were from Boehringer Mannheim and New England Biolabs (Beverly, MA).

*Construction of Cellubrevin-Ig and Other Plasmids*—Cb was polymerase chain reaction-amplified from a rat basophilic leukemia cDNA library (courtesy of Dr. Brian Seed, Massachusetts General Hospital) with primers (5′-CGCGGGAAGCTTGCCGCCACCATGTCTACAGGG-GTGCCT-3′ and 5′-CGCGGGGGATCCGAGACACACCACACAAT-3′), which allowed isolation of full-length Cb sequence with 5′ *Hin*dIII and 3′ *Bam*HI restriction sites for cloning into the pCD2B$\gamma$1 expression vector (courtesy of Dr. Brian Seed). This created an in-frame fusion of Cb to the CH2 and CH3 domains of human IgG after its hinge region. The resulting Cb-Ig construct was then transferred to the pCD43/hsfi$^-$ vector via *Hin*dIII and *Hpa*I sites for stable transfection in COS cells. pCD43/hsfi$^-$ (from Dr. Brian Seed) is a pCDM8-derived plasmid that contains CD43 in the stuffer region, confers resistance to hygromycin B, and has the SV40 origin of replication inactivated at the *Sfi*I site. Untagged Cb was amplified similarly with an additional stop codon in the antisense primer and cloned into the pcDNA3 vector (Invitrogen, San Diego, CA).

Organelle markers were constructed by attaching epitope tags to marker sequences containing the organelle targeting signals. The catalytic domain of UDP-glucuronyltransferase (UDPGT) was replaced with the CD4 epitope to generate CD4-UDPGT (courtesy of Dr. Brian Seed); the cytoplasmic dilysine motif of UDPGT targets this construct to the ER. The full coding sequences of galactosyltransferase (GalT) and furin have been appended with a Flag epitope tag at the COOH terminus to generate GalT-Flag and furin-Flag. GalT sequence with 5′ *Hin*dIII and 3′ *Xho*I sites was isolated by polymerase chain reaction amplification from a human liver cDNA library with the primers 5′-CGCGGGAAGCTTGCCACCATGAGGCTTCGGGAGCCG-3′ and 5′-CGCGGGCTCGAGGCTCGGTGTCCCGATGTC-3′; the ends of a mouse furin cDNA (pAGEFur, courtesy of Dr. K. Nakayama, University of Tsukuba, Ibaraki, Japan) were similarly modified by the primers 5′-CGCGGGAAGCTTGCCACCATGGAGCTGAGATCCTGG-3′ and 5′-CGCGGGCTCGAGAGGGGCGCTCTGGTCTTT-3′. Both products were inserted via 5′ *Hin*dIII and 3′ *Xho*I sites into the pCDM8-C-Flag vector, which contained the Flag epitope sequence for in-frame insertion of the tag at the C terminus.

*Transfections and Generation of Cell Lines Stably Expressing Cb-Ig*—COS-7 cells were grown in DMEM (BioWhittaker, Walkersville, MD) supplemented with 10% fetal calf serum and under 5% $CO_2$ atmosphere. CHO TRVb1 cells stably transfected with human Tf receptor (courtesy of Dr. T. E. McGraw, Cornell University Medical School, New York, NY) were grown in Ham's F-12 medium (Life Technologies, Inc.) supplemented with 10% fetal calf serum and under 5% $CO_2$ atmosphere. To isolate stable transfectants, semiconfluent cells in six-well plates were transfected with 1 $\mu$g of Cb-Ig/hsfi$^-$ using the lipofectamine procedure (Life Technologies), transferred to 10-cm dishes the next day, and subjected to selection with 200 $\mu$g/ml hygromycin B at 48 h post-transfection. Clones were screened by indirect immunofluorescence. Organelle markers were transiently transfected with the DEAE-dextran protocol of Seed and Aruffo (25).

*Immunofluorescence and Laser Scanning Confocal Microscopy*—Cells were washed twice with PBS, fixed in 3.7% paraformaldehyde for 20 min, and permeabilized in ice-cold 100% methanol for 20 s. Incubation for 15 min in 1% BSA/PBS preceded staining with the primary antibodies for 1 h and the secondary antibodies for 30 min. Washed coverslips were mounted on slides with a non-bleach reagent (KPL mounting media from Kirkegaard and Perry Labs, Inc. (Gaithersburg, MD) or 2.5% DABCO in 80% glycerol/PBS). A Zeiss Axiophot (Oberkochen, Germany) microscope with a × 63 objective was used for indirect immunofluorescence. For laser scanning confocal microscopy, cells were analyzed using a krypton/argon laser coupled with a Bio-Rad MRC1000 attached to a Zeiss Axioplan (Oberkochen, Germany) microscope with a Leitz Plan Apo × 63 oil/NA 1.4 objective. Separate excitation lines and emission filters were used for each fluorochrome (FITC, 488 nm (excitation) and 522DF32 (emission); Texas Red, 568 nm (excitation) and 605DF32 (emission)). Single optical sections separated by 0.54 $\mu$m were collected sequentially for each fluorochrome. Confocal images were background-subtracted, merged using the Confocal Assistant software program, and processed with Adobe Photoshop software. For quantitation, red, green, or yellow endosomes from merged 0.5-$\mu$m optical sections were counted by visual inspection of the enlarged image on a computer monitor. The following dilutions of antibodies were used: FITC-conjugated goat anti-human IgG, 1:25 (Cappel, Durham, NC); mouse anti-CD4 (Ortho Diagnostic Systems, Raritan, NJ), 1:500; mouse anti-Flag, 1:100 (Eastman Kodak Co.); Rh-conjugated goat anti-mouse IgG, 1:50 (Kirkegaard and Perry Labs); rabbit anti-Cb, 1:100 (courtesy of Dr. Reinhard Jahn, Max Planck Institute for Biophysical Chemistry); FITC-conjugated goat anti-rabbit IgG, 1:50 (Kirkegaard and Perry Labs).

*Uptake of Labeled F(ab) and Transferrin*—For continual uptake experiments, cells were washed twice with PBS and incubated for 2 h at 37 °C in DMEM containing 100 $\mu$g/ml of FITC-conjugated goat anti-human IgG F(ab) fragment (Cappel), 100 $\mu$g/ml Rh-transferrin (Molecular Probes, Inc., Eugene, OR), or 100 $\mu$g/ml Texas Red transferrin (Molecular Probes), and 1% BSA. Following this, the coverslips were washed three times with 10 mM acetic acid in PBS, fixed, and mounted. For pulse-chase experiments, cells were washed twice and incubated on ice for 20 min in serum-free DMEM supplemented with 1% BSA and 100 $\mu$g/ml of FITC-conjugated goat anti-human IgG F(ab) fragment. Following three washes to remove unbound antibody, the cells were either fixed immediately or returned to normal growth conditions for a 4-h chase. 100 $\mu$g/ml Rh-transferrin was added to the chase media to co-localize internalized antibody with endocytic structures. Surface-bound transferrin was removed with three washes of 10 mM acetic acid in PBS before fixation and viewing. For fluorescence ratio imaging experiments, the recycling endosomes were labeled with FITC-F(ab) in DMEM containing 10% serum, chased for 2–12 h, and washed with Ringer's solution (described below). For imaging the transferrin compartment, cells were serum-starved for 30 min in DMEM with 1% BSA and then loaded with FITC-Tf (50 $\mu$g/ml, Molecular Probes) in 1% BSA/DMEM for 2–5 h. Acetylstrophanthidin or bafilomycin was added to the media after the first hour. There was a nominal chase (~10 min) in the absence of Tf at room temperature while the coverslips were prepared for imaging.

*Fluorescence Ratio Imaging of Cytosolic and Endosomal pH*—Endosomal compartments labeled with F(ab)- or Tf-FITC and cytosol labeled with 2 $\mu$M BCECF-AM (Molecular Probes) were monitored in separate experiments using digitally processed fluorescence ratio imaging. Coverslips (22 mm diameter) with dye-loaded cells were placed in an open perfusion chamber on an inverted IM35 Zeiss microscope. Fluorescence measurements from up to 16 cells were made during each experiment. A × 40 or × 60 oil immersion objective (Zeiss) and either a × 1 (cytosol) or × 6.3 field objective (organelles) was used to magnify the images before transmission to the camera. A low light level DAGE 68 SIT camera collected (through a 530-nm band pass filter) emission images of the cells during excitation at 490 and 440 ± 5 nm (Omega Optical, Brattleboro VT). Filters were changed with a Lambda 10−2 filter wheel (Sutter Instruments, Novato CA). Separate images for each wavelength were averaged over eight frames by a digital image processor (Axon Image Lightning, Axon Instruments, Foster City CA) and subsequently converted pixel by pixel to a ratio image. Experimental parameters such as data collection rate (one ratio image every 5–60 s), changing the filter wheel and opening/closing the shutter were controlled by a 133-MHz Pentium computer (Gateway 2000) running Axon's Imaging Workbench. The ratio images were displayed in pseudocolor. Data were collected by electronically selecting regions of the image for quantitation. Cytosolic measurements were made from entire cells. For or-

ganelles, only the brightest perinuclear regions were selected. FITC fluorescence at 490 nm increases with pH, while fluorescence at 440 nm is nearly insensitive to pH. Problems due to photobleaching and dye loss were minimized by reducing the intensity (with neutral density filters), duration of illumination, and number of images collected.

*Perfusion of Solutions during pH Measurements*—Ringer's solution contained 141 mM NaCl, 2 mM KCl, 1.5 mM $K_2HPO_4$, 1 mM $MgSO_4$, 10 mM glucose, 2 mM $CaCl_2$, 10 mM HEPES, pH 7.4. Calibration solutions contained 70 mM KCl, 70 mM NaCl, 1 mM each $K_2HPO_4$ and $KH_2PO_4$, 1.3 mM $MgSO_4$, 10 mM glucose, 1 mM $CaCl_2$, and 10 mM HEPES or 10 mM MES, adjusted to various pH values with NaOH and KOH. HEPES was used for solutions with pH $>$ 6.5, and MES was used for solutions with pH $\leq$ 6.5.

*Calibration of BCECF and FITC Fluorescence in Terms of pH*—An *in situ* calibration was performed following each experiment to convert 490-/440-nm values to pH. Calibration solutions containing a 5–10 $\mu$M concentration of the $K^+/H^+$ exchange ionophore nigericin and a 5–10 $\mu$M concentration of the $Na^+/H^+$ exchange ionophore monensin were perfused over cells. By using these solutions, we made no assumptions about $Na^+$ and $K^+$ concentrations within cytosol or organelles and allowed the equilibration of $Na^+$ and $K^+$ to drive the equilibration of $H^+$. At least four solutions at various pH values (8.0, 7.5, 7.0, 6.5, 6.0, 5.5, and/or 5.0) were used per calibration. For each cell and organelle, a calibration curve was generated, the data were fit to a sigmoidal curve with Graphpad (San Diego, CA), and the resulting fit was used to convert the ratio to pH values using the equation $pH = pK + \log((R - R_{min})/(R_{max} - R))$, where $R$ is the ratio, $R_{min}$ and $R_{max}$ are the minimum and maximum values determined from the fit, and p$K$ is the p$K_a$ determined from the fit. Experimental data were compared using unpaired Student's $t$ test (two-tailed). All data are presented as mean ± S.E. Differences were considered significant if $p < 0.05$.

## RESULTS

*Experimental Strategy*—Our methodology for measuring the pH of recycling endosomes in living cells is outlined in Fig. 1. We placed a luminal epitope tag on Cb by extending its C terminus with the monomeric constant region of human IgG heavy chain. When this fusion construct (Cb-Ig) appeared at the cell surface, the IgG epitope was exposed to the external medium and could therefore be tagged by the exogenous addition of FITC-conjugated antibodies. The bound antibody subsequently hitch-hiked on the cycling protein and at steady state resided in the intracellular location of its escort protein. Organelle pH measurements were then made in single living cells using the pH sensitivity of the fluorescein moiety and digital imaging microscopy. Measurements were made over a sustained time and under a variety of conditions without the temporal limitations of using Tf-FITC, which is present only transiently in the recycling endosomes.

*Cb-Ig Localizes to the Recycling Endosomes*—A stable clone of COS-7 cells expressing Cb-Ig was isolated. To confirm that the fusion construct was properly targeted to the recycling endosomes, we used indirect immunofluorescence microscopy to colocalize Cb-Ig with markers for the ER, Golgi, *trans*-Golgi network (TGN), and endosomes. The ER, Golgi, and TGN were visualized by transient transfection with epitope-tagged constructs specifically targeted to these compartments: CD4-UDPGT (ER), galactosyltransferase-Flag (*trans*-Golgi), and furin-Flag (TGN) (see "Experimental Procedures"). Endosomes were labeled by a 2-h incubation in media containing 100 $\mu$g/ml Rh-Tf.

Cells were fixed, permeabilized, and doubly stained with antibodies against both human IgG on Cb-Ig and the epitope tag on the transfected organelle marker. Cb-Ig was found at the cell surface and in a perinuclear area (Fig. 2, *B*, *D*, *F*, and *H*), similar to that reported for unmodified Cb in CV-1, CHO, and rat brain glial cells (17–19). The distribution of Cb-Ig clearly did not coincide with the ER marker CD4-UDPGT, which was found in a branching, tubular network that extended throughout the cytoplasm but was most concentrated around the nucleus (Fig. 2*A*). Cb-Ig staining also differed from the Golgi

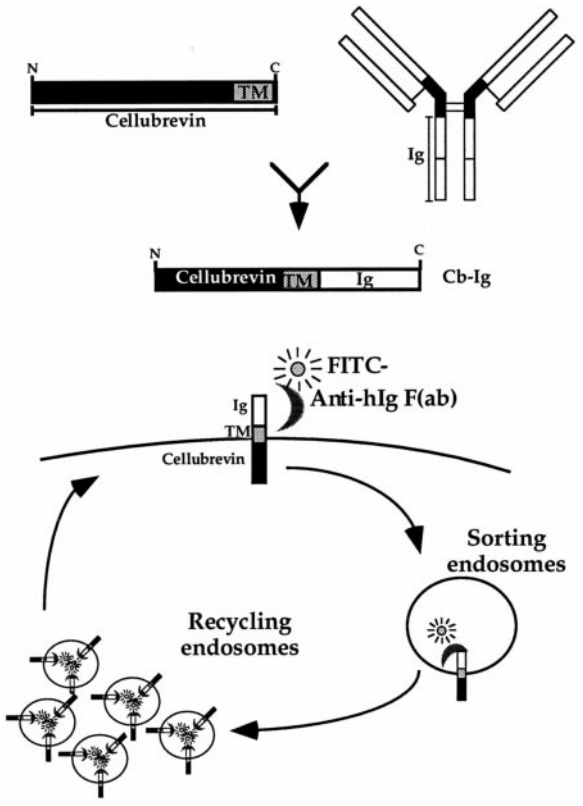


FIG. 1. **Schematic representation of Cb-Ig construction and targeting in living cells.** *Top*, a full-length rat Cb was fused in frame to the CH2 and CH3 domains of human IgG. The resulting Cb-Ig construct thus contained a luminal IgG epitope tag following the transmembrane (*TM*) domain of Cb. *Bottom*, Cb-Ig can be visualized in living cells by the addition of FITC-conjugated anti-hIgG F(ab) antibodies to the incubation medium. The continual cycling of Cb-Ig between the endosomes and plasma membrane results in the transient exposure of the IgG tag to the extracellular medium. When this occurs, the FITC-F(ab) antibodies bind to the epitope and travel with Cb-Ig through the endosomal system. Since in the steady state Cb-Ig resides in the recycling endosomes, the fluorescent signal arises predominantly from this location.

(GalT-Flag, Fig. 2*C*) and TGN (furin-Flag, Fig. 2*E*), two well defined tubular compartments that often formed bulbous, circular, and semicircular patterns in the perinuclear region of these cells. The overlapping but clearly distinct distributions of Cb-Ig, GalT-Flag, and furin-Flag was expected, as many organelles are positioned near the cell center (26). In contrast to the other markers, Rh-Tf (Fig. 2*G*) labeled a distinct pericentriolar spot which co-localized with Cb-Ig. This perinuclear localization of Tf has been used to define the recycling endosomes (1, 4, 11). We therefore concluded that, like native Cb, the Cb-Ig fusion construct was targeted to the recycling endosomes.

*Cycling of Cb Allows Antibody Uptake in Live Cells*—We further investigated the trafficking of Cb-Ig with a series of antibody uptake studies. Untransfected (Fig. 3, *A* and *B*) and Cb-Ig-transfected (Fig. 3, *C–F*) COS-7 cells were incubated in medium containing Rh-Tf and FITC-conjugated anti-IgG F(ab) fragment antibodies, and the patterns of F(ab) and Tf fluorescence were compared. A monovalent F(ab) fragment was used to ensure that the added antibody did not induce cross-linking of Cb-Ig. After a 2-h incubation in the continual presence of antibodies at 37 °C, Cb-Ig-transfected cells showed clear labeling of an organelle that was similar to that observed in the fixed and stained cells (compare Fig. 3*C* with Fig. 2). No fluorescence was detected in untransfected COS-7 cells (Fig. 3*A*), demonstrating that F(ab) antibody uptake was an epitope-mediated event and that "background" fluorescence resulting

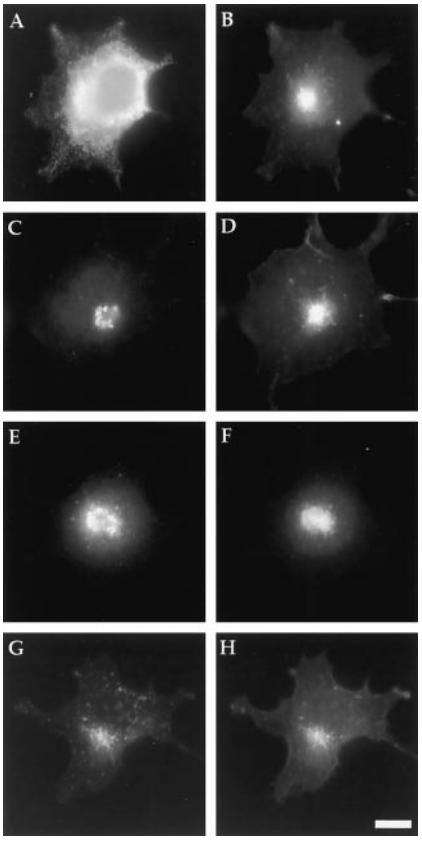


FIG. 2. **Localization of Cb-Ig in stably transfected COS-7 cells.** The steady-state distribution of Cb-Ig in a stably transfected cell line was examined by comparing its distribution with transiently transfected, epitope-tagged organelle markers. *A–F*, Cb-Ig is targeted to perinuclear structures distinguishable from compartments of the secretory pathway. Cells were fixed and permeabilized 48 h post-transfection and doubly stained for Cb-Ig (*B*, *D*, *F*) and the ER marker CD4-UDPGT (*A*), the Golgi marker GalT-Flag (*C*), or the TGN marker furin-Flag (*E*). FITC-goat anti-hIgG was used to visualize Cb-Ig, and the co-transfected markers were visualized with either mouse anti-CD4 or mouse anti-Flag followed by Rh-goat anti-mouse IgG. *G–H*, Cb-Ig and Tf were localized to the same perinuclear region characteristic of the recycling endosomes. Endosomes were labeled for 2 h with 100 $\mu$g/ml Rh-Tf (*G*) before fixation and staining with FITC goat anti-hIgG to localize Cb-Ig (*H*). *Bar*, 10 $\mu$m.

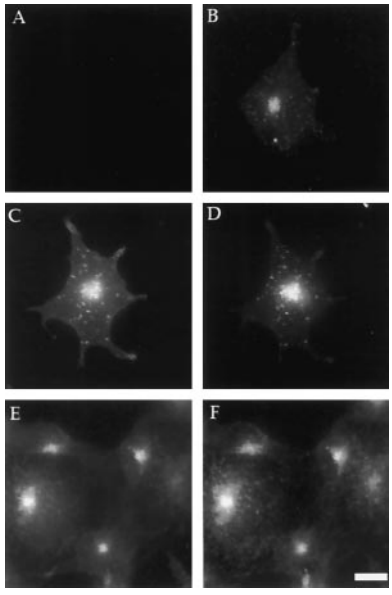


FIG. 3. **Labeling the Cb-Ig compartment in live cells by antibody uptake.** *A–D*, antibody uptake is dependent on the expressed Ig-epitope. Untransfected cells (*A*, *B*) and cells stably transfected with Cb-Ig (*C*, *D*) were incubated in medium containing 100 $\mu$g/ml FITC-goat anti-hIgG F(ab) fragment (*A*, *C*) and Rh-Tf (*B*, *D*). Cells were fixed after a 2 h 37 °C incubation in the continual presence of labels. Only the transfected cells (*C*) take up FITC-F(ab). *E* and *F*, pulse-chased antibodies accumulate in the perinuclear recycling endosomes. Cells stably transfected with Cb-Ig were pulse-labeled with 100 $\mu$g/ml FITC-goat anti-hIgG F(ab) on ice for 20 min. F(ab) was removed, and the cells were chased at 37 °C for 4 h in medium containing 100 $\mu$g/ml Rh-Tf. Endocytosed FITC-F(ab) fragment (*E*) was concentrated in the recycling endosomes as was Rh-Tf (*F*). *Bar*, 10 $\mu$m.

from fluid phase endocytosis of the antibody was minimal. In Cb-Ig-transfected cells, FITC-F(ab) and Rh-Tf were found together in vesicles dispersed throughout the cytoplasm and in the perinuclear recycling endosomes (Fig. 3, *C* and *D*). Some bound antibody was also present at the cell surface (Fig. 3*C*). As assessed by indirect immunofluorescence and cytofluorometry, the FITC signal was attenuated when cells were preincubated with unconjugated anti-hIgG F(ab) antibodies for 2 h at 37 °C before FITC-F(ab) labeling (data not shown). These results demonstrated that, in addition to proper targeting, the fusion construct continually cycled through the endosomal system in a manner analogous to that presumed for native Cb.

The recycling endosomes were also labeled with a pulse-chase protocol. A 20-min incubation on ice with FITC-conjugated goat anti-human IgG F(ab) antibodies labeled the plasma membrane of transfected cells, whereas no fluorescent signal could be detected in untransfected cells. After a 4-h chase at 37 °C, the surface label had dissipated and was replaced by a perinuclear stain that colocalized with Rh-Tf (Fig. 3, *E* and *F*). Surface and peripheral endosome staining was not visible, presumably because the majority of FITC-labeled Cb-Ig accumulated in the recycling endosomes at steady state. Labeling of the recycling endosomes was apparent within 45 min of chase and was still visible after 24 h (data not shown).

*Laser Scanning Confocal Microscopy Distinguishes Endosomes Labeled by Tf and Cb*—The distributions of Cb-Ig and Rh-Tf were examined in greater detail with the use of laser scanning confocal microscopy (Fig. 4). After a 3-h incubation with 100 $\mu$g/ml of Texas Red Tf, cells were fixed, permeabilized, and stained with FITC goat anti-hIgG antibodies. Representative merged images from single optical sections are shown. In contrast to the results obtained with indirect immunofluorescence, Cb-Ig and Tf could be visualized in separate pericentriolar vesicle populations. These differences were most obvious near the bottom or top of the cell, but differences could also be visualized in the middle sections where extensive colocalization was also present (Fig. 4*A*). The same result was obtained when Cb-Ig was localized by FITC-F(ab) antibody uptake (Fig. 4*B*) and when endogenous Cb was visualized in untransfected COS-7 cells (Fig. 4*C*). These results indicated that neither the luminal IgG epitope nor F(ab) internalization was affecting the localization of Cb-Ig. Observation of cells stained with a single fluorophore (either Texas Red Tf or FITC-conjugated anti-hIgG antibodies) demonstrated that bleed-through was not occurring in the optical sections (data not shown).

Microtubule depolymerization leads to the dispersal of many organelles throughout the cytoplasm (6, 15, 26, 27) and would thus allow for a more definitive examination of Cb/Tf codistribution. We therefore repeated our experiments in cells treated with the microtubule depolymerizing agent nocodazole. As shown in Fig. 4, *D–F*, some degree of colocalization persisted in nocodazole-treated cells. This was observed when Cb-Ig was visualized by postfixation staining (Fig. 4*D*) or by FITC-F(ab) antibody uptake (Fig. 4*E*). Partial colocalization was also seen in COS-7 cells transiently transfected with an untagged Cb (Fig. 4*F*). Transient transfection of untagged Cb was required, because the distribution of endogenous Cb could not be de-

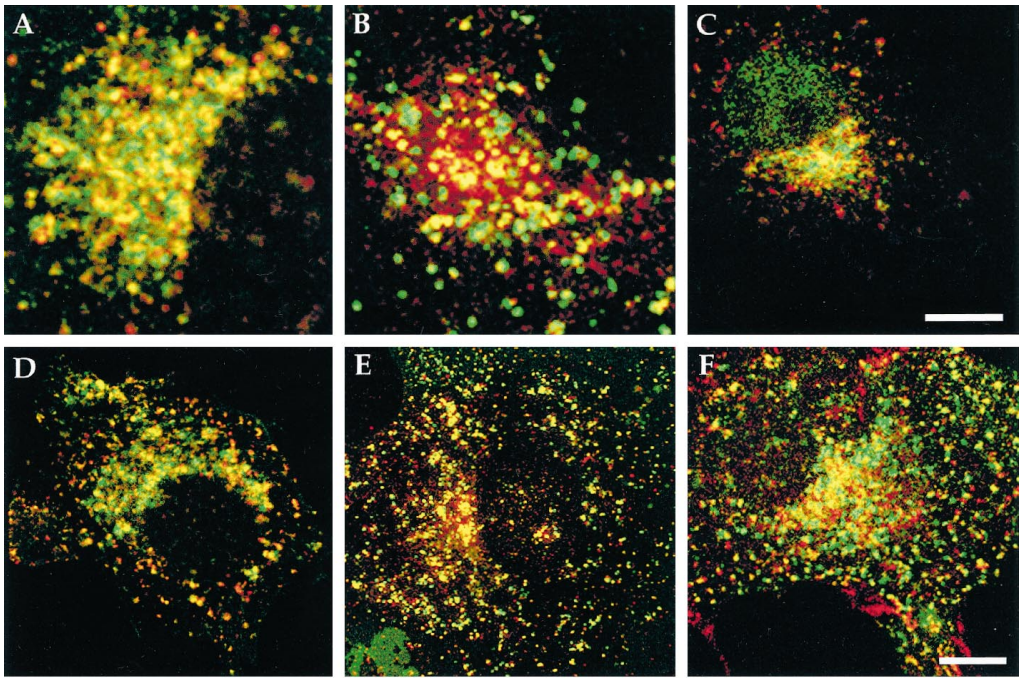


FIG. 4. **Localization of Cb and Tf assessed by laser scanning confocal microscopy.** Cb and Tf are heterogeneously distributed among the recycling endosomes. Representative merged images from single 0.5-$\mu$m optical sections are shown. For all conditions, Tf was visualized by a 3-h incubation with 100 $\mu$g/ml Texas Red Tf. *A–C*, Cb-Ig was visualized in stably transfected COS-7 cells by either postfixation staining with FITC goat anti-hIgG antibodies (*A*) or by a 3-h incubation with 100 $\mu$g/ml FITC goat anti-hIgG F(ab) antibodies (*B*). Endogenous Cb was visualized in untransfected COS-7 cells by postfixation staining with rabbit anti-Cb antibodies followed by FITC goat anti-rabbit IgG antibodies (*C*). *D–F*, cells were treated with 20 $\mu$M nocodazole for 1 h prior to fixation. Cb-Ig was visualized in stably transfected COS-7 cells by either postfixation staining with FITC goat anti-hIgG antibodies (*D*) or by a 3-h incubation with 100 $\mu$g/ml FITC goat anti-hIgG F(ab) antibodies (*E*). Transiently transfected, untagged Cb was visualized in COS-7 cells by postfixation staining with rabbit anti-Cb antibodies followed by FITC goat anti-rabbit IgG antibodies (*F*). Cb-enriched (*green*), Tf-enriched (*red*), and Cb/Tf intermixed (*yellow*) endosomes could be observed in all optical sections under any of the given conditions. *Bar* in *A–C*, 5 $\mu$m; *bar* in *D–F*, 10 $\mu$m.

TABLE I

*Distribution of endosomes containing Cb, Cb and Tf, and Tf*

The degree of overlap between Cb and Tf is shown. Images such as those in Fig. 4 were visually screened for green (Cb-enriched), yellow (Cb- and Tf-intermixed), or red (Tf-enriched) vesicles. At least 650 endosomes from five or more cells were quantitated for each condition and section. Results are presented as the percentage of endosomes that are Cb-enriched, Cb and Tf intermixed, and Tf-enriched. Comparisons were made between Tf and endogenous Cb visualized by postfixation staining (Cb fix), untagged transfected Cb visualized by postfixation staining after nocodazole treatment (nocodazole/Cb fix), Cb-Ig at steady state with or without nocodazole treatment (Cb-Ig fix and nocodazole/Cb-Ig fix), or internalized antibodies bound to Cb-Ig with or without nocodazole treatment (F(ab) and nocodazole/F(ab)). In cells prepared without nocodazole treatment, only perinuclear vesicles were considered. Middle sections were defined as those images in which the nucleus and cell body were clearly defined.

| Marker and labeling condition | Cb-enriched/Cb and Tf/Tf-enriched | | |
|---|---|---|---|
| | Bottom cell section | Middle cell section | Top cell section |
| | % | | |
| Cb fix | 37/13/50 | 46/28/26 | 45/32/23 |
| Cb-Ig fix | 40/17/42 | 44/27/29 | 55/21/24 |
| F(ab) | 40/22/38 | 43/25/31 | 48/23/30 |
| Nocodazole/Cb fix | 32/21/47 | 45/29/25 | 51/21/27 |
| Nocodazole/Cb-Ig fix | 47/23/30 | 51/28/22 | 61/21/19 |
| Nocodazole/F(ab) | 52/17/31 | 44/32/24 | 58/22/20 |

tected over background fluorescence in nocodazole-treated cells. Transfection did not alter the steady state distribution of Cb (data not shown) and allowed individual structures to be resolved in nocodazole-treated cells. The partial codistribution of Cb and Tf in both untreated and nocodazole-treated cells thus indicated that the proteins were targeted to overlapping but distinct subpopulations of recycling endosomes.

The percentage of Cb-enriched (*green*), intermixed (*yellow*), and Tf-enriched (*red*) endosomes was determined by visual inspection of merged optical sections such as those shown in Fig. 4 (Table I). Since the degree of overlap varied with the cell section, values are given for bottom, middle, and top regions of the cell. Only perinuclear vesicles were counted in cells prepared without nocodazole treatment. Several trends could be ascertained from Table I: (i) in all optical sections, only 20–30% of endosomes showed intermixing of Cb and Tf, the rest being composed of Cb- or Tf-enriched vesicles; (ii) the percentage of Cb-enriched endosomes increased as confocal sectioning progressed from the bottom to the top of the cell; (iii) the percentage of Tf-enriched endosomes decreased as confocal sectioning progressed from the bottom to the top of the cell; and (iv) Cb-enriched vesicles were more predominant than Tf-enriched or intermixed endosomes in almost all optical sections. These general trends applied to all tested conditions and further documented the heterogeneous distributions of Cb and Tf in the recycling endosomes.

*$pH_{Cb}$ Is Lower Than $pH_{Tf}$*—The epitope specificity of the F(ab) antibody uptake in conjunction with the 4 °C pulse labeling and 37 °C chase resulted in specific labeling of the Cb-Ig-containing recycling endosomes (Fig. 3*E*). We used this protocol for *in vivo* pH measurements. Briefly, cells chased for 2–12 h were set into an open perfusion chamber and alternately illuminated with 490- and 440-nm light. An example is shown in Fig. 5, *A* and *B*. The resulting ratio image (490/440 nm) from the bright perinuclear spot estimated organelle pH (Fig. 5*C*). Raw ratio data from three of the cells in Fig. 5, *A–C*, are shown in Fig. 6*A*. Organelle viability was demonstrated by the instantaneous alkalization resulting from perfusion with Ringer's solution containing 30 mM $NH_4Cl$. Following treatment with $NH_4Cl$, membranes were permeabilized with nigericin and monensin in equimolar $Na^+$ and $K^+$ with varying pH values.

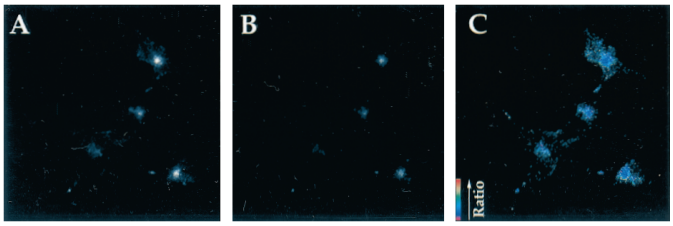


FIG. 5. **Fluorescent ratio imaging of $pH_{Cb}$.** Cb-Ig cells were incubated with 100 $\mu$g/ml of FITC-goat anti-hIgG F(ab) for 30 min at 4 °C and then chased for 5 h at 37 °C. Cells were illuminated with either 490- (*A*) or 440-nm (*B*) wavelength light, and images were captured with a low light level DAGE 68 SIT camera. A pixel by pixel ratio image was created and displayed in pseudocolor (*C*). "Hotter" colors in the ratio image indicate increasing pH.

The calibration data from this experiment are presented in Fig. 6*B*. The ratio values at a given pH were stable for many minutes and provided a consistent reading; multiple exposures to the pH 6.5 solution produced the same organelle ratio value. Using this calibration curve, we estimated an average $pH_{Cb}$ of 6.2 for the three cells in Fig. 5. An apparent $pK_a$ of 6.6 for FITC-F(ab) was derived from the calibration data obtained from all experiments performed in both COS-7 cells (Fig. 6*C*) and CHO cells stably transfected with Cb-Ig (not shown). The $pH_{Cb}$ distribution from all experiments performed in COS-7 cells (Fig. 6*D*, *solid bars*) showed a wide range of recorded values, from 5.2 to 6.6 with an average of 6.1 ± 0.05 ($n$ = 35 cells; 12 experiments). An identical $pH_{Cb}$ of 6.1 ± 0.05 ($n$ = 16 cells; four experiments) was measured in CHO cells stably transfected with Cb-Ig (Fig. 6*E*, *solid bars*).

Since the values obtained using Cb-Ig were considerably lower than previous data obtained with FITC-Tf, we repeated the pH measurements using FITC-Tf loaded into the same cell lines. Cells were incubated with FITC-Tf for 2–5 h and then chased for 10 min in Ringer's solution at room temperature. Imaging of the perinuclear recycling endosomes again produced an array of values (Fig. 6*D*, *hatched bars*), although both the range (5.6–7.2) and average $pH_{Tf}$ of 6.5 ± 0.05 ($n$ = 46 cells; six experiments) were significantly more alkaline ($p < 0.05$) in the Tf-labeled compartment. A similar $pH_{Tf}$ of 6.6 ± 0.06 ($n$ = 16 cells; five experiments) was obtained in CHO cells stably transfected with human Tf receptor and Cb-Ig (Fig. 6*E*, *hatched bars*). A broad $pH_{Tf}$ distribution has previously been observed by others recording the $pH_{Tf}$ of individual endosomes (22). The average pH obtained with either Cb-Ig or Tf thus represented a range of values that varied from cell to cell and, most likely, from endosome to endosome.

*Bafilomycin and Ouabain Exert Different Effects on $pH_{Cb}$ and $pH_{Tf}$*—Previous Tf-based studies have reported that endosomal pH is maintained by a $H^+$-ATPase and regulated by $Na^+/K^+$-ATPase activity (21–24, 28, 29). In order to test whether these mechanisms were active in the Cb-Ig-containing recycling endosomes, we applied bafilomycin and either ouabain or acetylstrophanthidin (a membrane-permeant ouabain analog) to COS-7 cells and determined the effect on endosomal pH. Treatment with 100 nM bafilomycin $A_1$, an inhibitor of the vacuolar-type $H^+$-ATPase, elicited an increase in $pH_{Cb}$. In the experiment shown in Fig. 7*A*, bafilomycin caused $pH_{Cb}$ to increase from 6.3 to 7.0. On average, bafilomycin treatment shifted $pH_{Cb}$ from 6.2 ± 0.08 to 6.7 ± 0.09 ($n$ = 10 cells; three experiments). We also measured the effect of bafilomycin on $pH_{Tf}$ (Table II); pretreatment of cells with 100 nM bafilomycin caused a more pronounced shift in $pH_{Tf}$ from 6.5 ± 0.05 to 7.7 ± 0.05 ($n$ = 18 cells; three experiments). The bafilomycin-induced alkalization to a $pH_{Tf}$ greater than 7.0 has been observed by others (23, 24, 29). These results demonstrated that both classes of recycling endosomes maintained a steady state pH by the continual action of a $H^+$-ATPase operating to counter a leak of proton equivalents. Similar conclusions about pH regulation in the endosomes, phagosomes, Golgi, and TGN have been published (30–33). It was possible that the recycling endosome pH might have been affected only indirectly by bafilomycin, due to an effect of the drug on cytosolic pH ($pH_c$). We therefore measured $pH_c$ in COS-7 cells using BCECF-AM. The average $pH_c$ (7.5 ± 0.03, $n$ = 53 cells; six experiments) in COS-7 cells was unaffected by bafilomycin (data not shown), so alkalization of the recycling endosomes was not due to a secondary effect arising from a change in $pH_c$. We concluded that recycling endosomes maintained their acidity due to the activity of an $H^+$-ATPase, while $pH_c$ was regulated by other mechanisms.

In contrast to bafilomycin, ouabain had no effect on $pH_{Cb}$ (Fig. 7*B*). Based on the speed with which Tf and bulk membrane enter the recycling endosomes (4, 10, 34), perfusion of labeled cells with ouabain should have inhibited the recycling endosome $Na^+/K^+$-ATPase within 5 min. Yet, as shown in Fig. 7*B*, ouabain had no effect on $pH_{Cb}$ over this time course. Treatment with 1 $\mu$M of the membrane-permeant $Na^+/K^+$-ATPase inhibitor acetylstrophanthidin also had no effect over 30–60 min (three experiments; data not shown). However, as shown in Table II, inhibition of the $Na^+/K^+$-ATPase by pretreatment with acetylstrophanthidin caused $pH_{Tf}$ to decrease; the average $pH_{Tf}$ of 6.5 obtained from FITC-Tf-loaded cells acidified to $pH_{Tf}$ 5.9 in cells pretreated with 1 $\mu$M acetylstrophanthidin. It thus appeared that Tf and Cb-Ig were targeted to overlapping perinuclear compartments that differed in both average pH and responses to inhibitors of $Na^+/K^+$-ATPase and $H^+$-ATPase activity.

We also examined the effects of altering endosomal pH on the cycling of Cb-Ig and Tf to the cell surface by quantitative assays using $^{125}$I-protein A and $^{125}$I-Tf. These studies showed that bafilomycin slowed trafficking of both Cb-Ig and Tf from the recycling endosomes to the plasma membrane, while ouabain and acetylstrophanthidin had no effect on either marker (data not shown).

## DISCUSSION

*"Targeted Fluorescence" Method to Study pH of the Recycling Endosomes*—The targeted fluorescence method is based on binding exogenously added fluorescent antibodies to specific "resident" proteins that cycle between the plasma membrane and their home organelle. We chose Cb because it is thought to cycle between recycling endosomes and the plasma membrane (17–19). Proper targeting of Cb-Ig to recycling endosomes was confirmed by colocalization with Rh-Tf but not with markers for the ER, Golgi, or TGN. Uptake of FITC-F(ab) antibodies was mediated by binding to Cb-Ig exposed at the surface (and not by bulk endocytosis), probably due to the fact that very low concentrations of FITC-F(ab) allowed specific labeling of the recycling endosomes (*e.g.* 100 $\mu$g/ml as opposed to 5–10 mg/ml required for fluid phase endocytosis (22, 24)). Preincubation with unlabeled F(ab) significantly reduced subsequent uptake of FITC-F(ab), demonstrating that Cb indeed cycled between endosomes and the plasma membrane. The "targeted fluorescence" strategy has also been useful for examining pH of the TGN and may be a general strategy for studying organelles containing proteins that cycle between the cytosol and the plasma membrane (33, 35).

We found that $pH_{Cb}$ ranged from 5.2 to 6.6 (mean $pH_{Cb}$ 6.1). FITC-Tf also showed a wide range of values, although both the range ($pH_{Tf}$ 5.6–7.2) and average (mean $pH_{Tf}$ 6.5) were significantly more alkaline than $pH_{Cb}$. A broad distribution (pH 5.5–7.2) has also been observed in endosomes labeled with fluorescein/rhodamine-Tf, although the majority fell within a

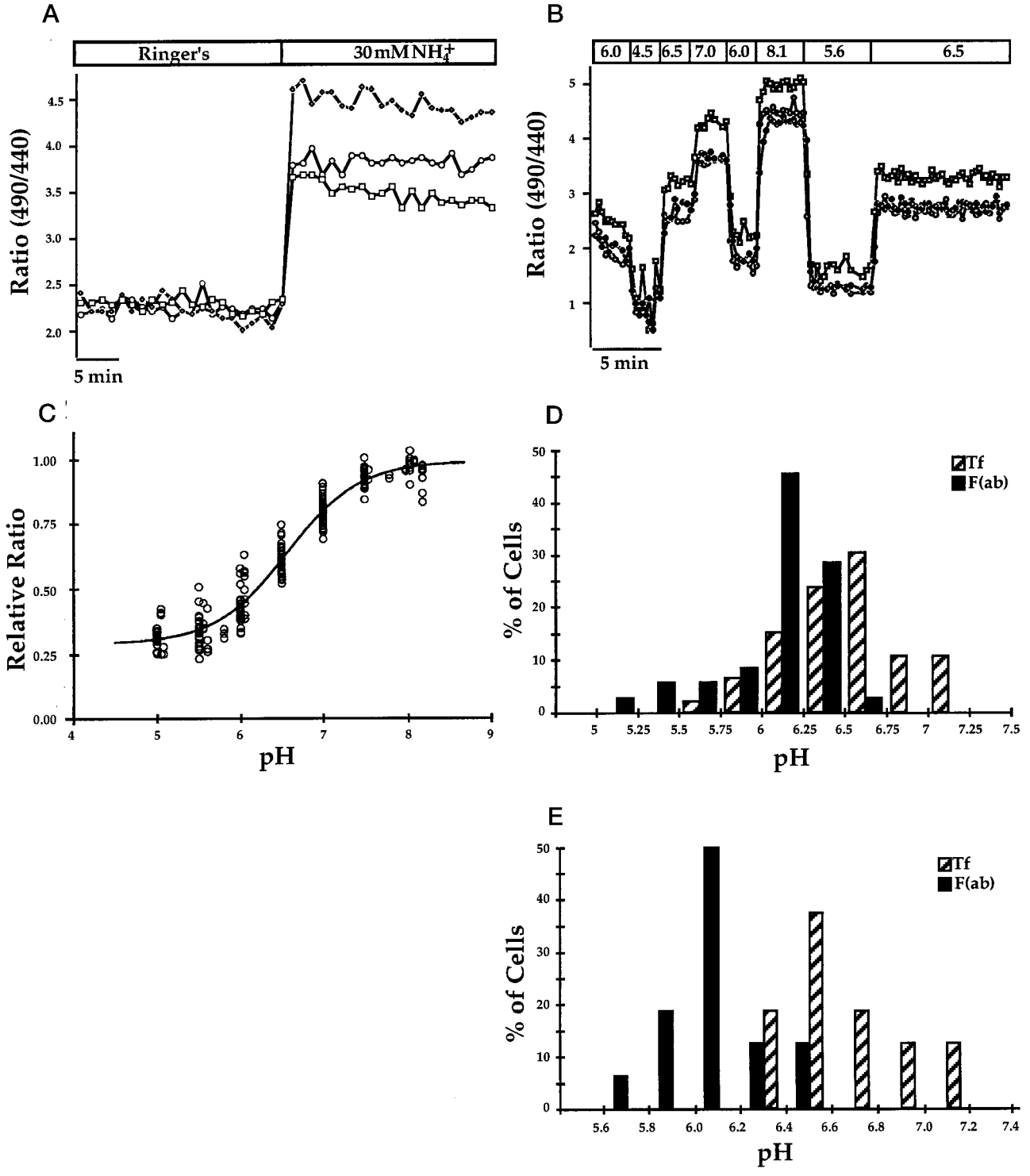


FIG. 6. **Quantitation of $pH_{Cb}$ and comparison with $pH_{Tf}$.** *A* and *B*, numerical data from three of the four cells in Fig. 5 are plotted *versus* time. $pH_{Cb}$ increased during a 30 mM $NH_4^+$ pulse, showing that membranes of the recycling endosomes were intact (*A*). Calibration data of cells shown in *A* indicated that the signals were stable for >20 min. Cells were pulsed with solutions at various pH values containing 10 $\mu$M nigericin and monensin(*B*). *C*, summary of all calibrations (35 cells). The 490-/440-nm fluorescence ratio for each cell was plotted *versus* pH of the calibration solution, and the maximum values from individual fits were set to 1. The raw calibration data were then expressed relative to the fitted maximum to allow comparison among experiments. These data indicated that the apparent $pK_a$ was ~6.6. *D* and *E*, frequency histogram of organelle pH in COS-7 (*D*) and CHO (*E*) cells. $pH_{Cb}$ was measured as in *A* and *B*, and $pH_{Tf}$ was measured as in Table II. Data represent a summary of all $pH_{Cb}$ and $pH_{Tf}$ measurements made and are expressed as a percentage of the total number of cells measured for each marker. For COS-7 cells, there were 35 measurements for the Cb compartment and 46 measurements for the Tf compartment; for CHO cells, there were 16 measurements for both the Cb and Tf compartment.

pH range of 6.0–6.5 (22, 24, 29). Rybak *et al.* (36) have proposed that variations in endosome size, shape, buffering capacity, and ion transport activity could account for this broad pH distribution. A wide pH range may not be limited to the endosomal system, since highly variable pH values in both the Golgi (32) and immature secretory vesicles (37) have also been reported.

D'Souza *et al.* (35) have also used Cb-targeted fluorescence to

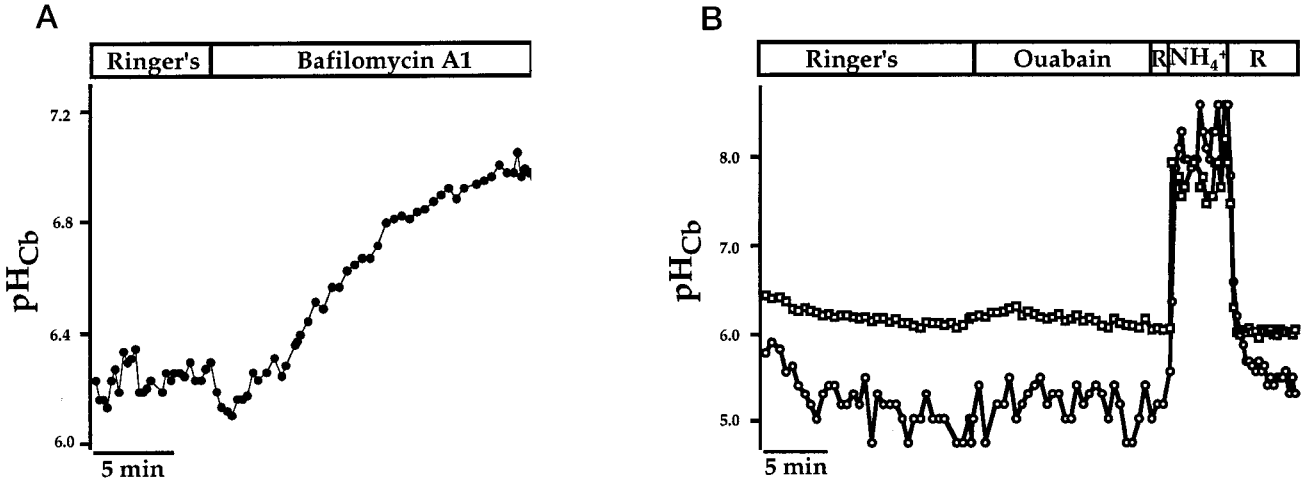


FIG. 7. **Effects of bafilomycin and ouabain on $pH_{Cb}$.** $pH_{Cb}$ is alkalinized by bafilomycin and is unaffected by ouabain. *A*, $pH_{Cb}$ was measured in COS-7 cells as described in the legend to Fig. 6. A representative trace is shown from a cell over which 100 nM bafilomycin was perfused. The cell rapidly alkalinized due to inhibition of the $H^+$-ATPase but remained intact as indicated by its continued responsiveness to $NH_4^+$ (data not shown). On average, bafilomycin treatment shifted $pH_{Cb}$ from 6.2 ± 0.08 to 6.7 ± 0.09 ($n$ = 10 cells; three experiments). *B*, there was no pH change when 100 $\mu$M ouabain was applied to the cells. Traces from two cells within the same dish are shown; they had different $pH_{Cb}$ values, but neither responded to ouabain treatment. *R*, Ringer's solution.

TABLE II
*Drug effects on $pH_{Tf}$*

The effect of bafilomycin and acetylstrophanthidin on $pH_{Tf}$ is shown. COS-7/Cb-Ig cells were incubated in 50 $\mu$g/ml FITC-Tf for 2–5 h. Drugs were added for 1–4 h prior to pH measurements. Acetylstrophanthidin (1 $\mu$M) acidified the compartment, whereas bafilomycin (100 nM) dramatically alkalinized the compartment. As FITC-Tf is rapidly transported out of the recycling endosomes, drug pretreatment was necessary in order to ensure that an effect could be seen before FITC-Tf exited the compartment. These measurements therefore represented an effect on the average $pH_{Tf}$ but did not show the real-time changes induced by inhibition of the $Na^+/K^+$-ATPase or $H^+$-ATPase. The control Tf data from Fig. 6*D* are presented for comparison.

| | Mean ± S.E. | No. of cells | No. of experiments |
|---|---|---|---|
| Control | 6.5 ± 0.05 | 46 | 6 |
| With 1 $\mu$M strophanthidin | 5.9 ± 0.06[a] | 23 | 3 |
| With 100 nM bafilomycin | 7.7 ± 0.05[a] | 18 | 3 |

[a] Statistical significance using Student's $t$ test ($p < 0.05$).

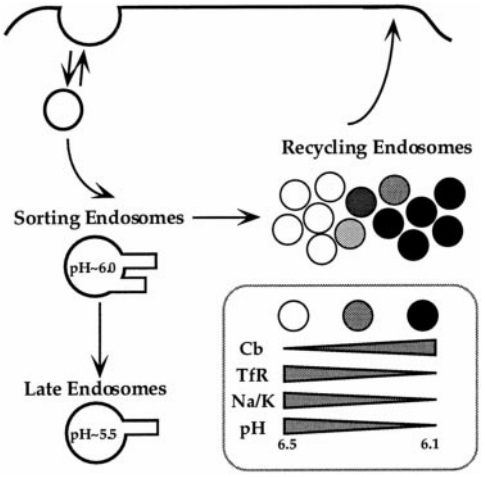


FIG. 8. **Model for the heterogeneous composition of the recycling endosomes.** Endocytosed molecules are transported from the plasma membrane to sorting endosomes (pH 6.0), whereupon ligands and receptors are dissociated. Soluble ligands continue to late endosomes (pH 5.5), while membrane proteins are sorted to the perinuclear recycling endosomes. Cb and Tf are partitioned into subpopulations of this compartment. The Tf-enriched subclass has an average pH of 6.5, which is generated by a $H^+$-ATPase and regulated by a $Na^+/K^+$-ATPase. In contrast, the Cb-enriched subclass has an average pH of 6.1, which is similarly generated by a $H^+$-ATPase but lacks detectable $Na^+/K^+$-ATPase activity. Inhibition of the $H^+$-ATPase also has a differential effect on the compartmental pH of the two subpopulations.

measure $pH_{Cb}$ in CHO cells lacking the $Na^+/H^+$ exchanger. Their reported value of $pH_{Cb}$ 6.7 contrasts with the $pH_{Cb}$ 6.1 we observed in both COS-7 and CHO cells. This discrepancy may be due to differences in wild-type *versus* $Na^+/H^+$ exchange-deficient CHO cells or could reflect an unexpected physiological effect on $pH_{Cb}$ induced by the "$H^+$ suicide" method for selecting $Na^+/H^+$ exchange-deficient cells. This difference deserves further attention.

*Differential Distribution of Cb and Tf among Recycling Endosomes*—Although Cb apparently co-localized with Rh-Tf, it became obvious that the two labels were in different subpopulations of endosomes. First, confocal microscopy demonstrated that the majority of labeled endosomes contained differing amounts of Cb-Ig and Tf (Fig. 4 and Table I). This difference was also observed with native Cb (Fig. 4 and Table I), thereby demonstrating the similar localization of native Cb and Cb-Ig. Second, pH measurements yielded distinct results depending on whether Cb-Ig or Tf was used as the organelle marker. Previous work using Tf as a recycling endosome marker recorded an average $pH_{Tf}$ of 6.4 (4, 22–24). We confirmed these findings in COS-7 and CHO cells but consistently found $pH_{Cb} < pH_{Tf}$. Furthermore, bafilomycin $A_1$ caused $pH_{Cb}$ to increase by 0.5 pH units to 6.7, while $pH_{Tf}$ increased 1.2 pH units to 7.7. Finally, acetylstrophanthidin caused $pH_{Tf}$ to decrease (also see Refs. 21–24), but neither ouabain nor acetylstrophanthidin affected $pH_{Cb}$, regardless of the initial $pH_{Cb}$ value.

A model summarizing our data (Fig. 8) proposes that recycling endosomes are heterogeneous, ranging between the two extremes of a highly enriched Tf subpopulation and a highly enriched Cb subpopulation. All occupy a perinuclear location, thereby leading to the gross colocalization of Tf and Cb (15, 17, 18). These endosomes utilize a $H^+$-ATPase to generate luminal acidity but have different pH values and $Na^+/K^+$-ATPase activity and can be segregated morphologically using nocodazole. The Cb population was more acidic and was not affected by $Na^+/K^+$-ATPase inhibitors, while the Tf population was somewhat more alkaline and was acidified by inhibitors of the $Na^+/K^+$-pump. The differential distribution of $Na^+/K^+$-ATPase activity between Tf- *versus* Cb-containing recycling endosomes may also be responsible for the difference in $pH_{Cb}$ and $pH_{Tf}$ after bafilomycin treatment; $Na^+/K^+$-pump activity could gen-

erate a positive membrane potential that would drive $H^+$ out of the Tf compartment, leading to a more alkaline pH than that found in the Cb-containing recycling endosomes, which appear to lack $Na^+/K^+$-ATPase activity. Either absence or regulation of the $Na^+/K^+$-ATPase activity could account for our $pH_{Cb}$ observations. Other channels and pumps are likely to play a role in pH homeostasis as well.

Previous data are also consistent with the proposal that recycling endosomes are heterogeneous. Daro *et al.* (15) showed that recycling endosomes contained both Tf and Cb; but one subpopulation contained Rab4, while another did not. In addition, Rab11 was found on both Tf-positive and Tf-negative recycling vesicles (16). Finally, cleavage and inactivation of Cb by tetanus toxin reduced Tf release by only 20–33% (18), although Cb's proposed role as a v-SNARE for trafficking of endosomal vesicles to the plasma membrane (17, 18, 38) would have predicted a complete block (39). Our model predicts that the 20–33% of tetanus toxin-sensitive Tf was present in the pool of recycling endosomes that contained both Tf and Cb (*e.g.* see Table I), while the 67–80% of Tf present in endosomes that did not contain Cb were insensitive to the toxin.

*Possible Function of Recycling Endosome Subpopulations*—Although we do not know the exact functions and trafficking patterns of the Tf and Cb endosome subpopulations, an intriguing possibility is that recycling endosomes act as a sorting station for targeting internalized proteins to the TGN. This idea could explain the apparent structural reorganization of the endosomal system that has been proposed for cells expressing a chimeric TGN38/TfR protein (TfR internalization motif replaced with the TGN38 YQRL targeting signal; see Ref. 40). The TGN38/TfR construct localized not to the TGN, but instead to a juxtanuclear structure that was morphologically distinct and significantly more acidic (pH 6.0) than the wild-type TfR-containing recycling endosomes (pH 6.5). In light of the work presented here, we propose an alternative explanation that the TGN38/TfR was targeted to the Cb-containing subpopulation of recycling endosomes that is present at all times. Further work will be required to elucidate the role of the Cb-containing recycling endosomes as a possible sorting station for targeting internalized proteins to the TGN.

*Acknowledgments*—We thank members of the Moore and Machen labs for critical reading of the manuscript, Amy Robinson for the figures, Dr. Brian Seed for providing the cDNA libraries and expression vectors used in this study, Dr. Kazuhisa Nakayama for supplying the furin plasmid, Dr. Robert Murphy for sharing his preprint with us, Dr. Duncan Stuart for technical assistance with the confocal microscope, and Axon Instruments for providing the imaging hardware and software.

REFERENCES

1. Gruenberg, J., and Maxfield, F. R. (1995) *Curr. Opin. Cell. Biol.* **7,** 552–563
2. Mellman, I. (1996) *Annu. Rev. Cell Dev. Biol.* **12,** 575–625
3. Hopkins, C. R. (1983) *Cell* **35,** 321–330
4. Yamashiro, D. J., Tycko, B., Fluss, S. R., and Maxfield, F. R. (1984) *Cell* **37,** 789–800
5. Griffiths, G., Back, R., and Marsh, M. (1989) *J. Cell Biol.* **109,** 2703–2720
6. Tooze, J., and Hollinshead, M. (1991) *J. Cell Biol.* **115,** 635–653
7. Stoorvogel, W., Strous, G. J., Geuze, H. J., Oorschot, V., and Schwartz, A. L. (1991) *Cell* **65,** 417–427
8. Klausner, R. D., Ashwell, G., van Renswoude, J., Harford, J. B., and Bridges, K. R. (1983) *Proc. Natl. Acad. Sci. U. S. A.* **80,** 2263–2266
9. Dautry, V. A., Ciechanover, A., and Lodish, H. F. (1983) *Proc. Natl. Acad. Sci. U. S. A.* **80,** 2258–2262
10. Dunn, K. W., McGraw, T. E., and Maxfield, F. R. (1989) *J. Cell Biol.* **109,** 3303–3314
11. Marsh, E. W., Leopold, P. L., Jones, N. L., and Maxfield, F. R. (1995) *J. Cell Biol.* **129,** 1509–1552
12. Nunez, M. T., Nunez-Millacura, C., Beltran, M., Tapia, V., and Alvarez-Hernandez, X. (1997) *J. Biol. Chem.* **272,** 19425–19428
13. Wilson, J. M., and Colton, T. L. (1997) *J. Cell Biol.* **136,** 319–330
14. Wei, M. L., Bonzelius, F., Scully, R. M., Kelly, R. B., and Herman, G. A. (1998) *J. Cell Biol.* **140,** 565–575
15. Daro, E., Sluijs, V. D., Galli, T., and Mellman, I. (1996) *Proc. Natl. Acad. Sci. U. S. A.* **93,** 9559–9564
16. Ullrich, O., Reinsch, S., Urbe, S., Zerial, M., and Parton, R. G. (1996) *J. Cell Biol.* **135,** 913–924
17. McMahon, H. T., Ushkaryov, Y. A., Edelmann, L., Link, E., Binz, T., Niemann, H., Jahn, R., and Sudhof, T. C. (1993) *Nature* **364,** 346–349
18. Galli, T., Chilcote, T., Mundigl, O., Binz, T., Niemann, H., and De Camilli, P. (1994) *J. Cell Biol.* **125,** 1015–1024
19. Chilcote, T. J., Galli, T., Mundigl, O., Edelmann, L., McPherson, P. S., Takei, K., and De Camilli, P. (1995) *J. Cell Biol.* **129,** 219–231
20. Sipe, D. M., and Murphy, R. F. (1987) *Proc. Natl. Acad. Sci. U. S. A.* **84,** 7119–7123
21. Cain, C. C., Sipe, D. M., and Murphy, R. F. (1989) *Proc. Natl. Acad. Sci. U. S. A.* **86,** 544–548
22. Zen, K., Biwersi, J., Periasamy, N., and Verkman, A. S. (1992) *J. Cell Biol.* **119,** 99–110
23. Johnson, L. S., Dunn, K. W., Pytowski, B., and McGraw, T. E. (1993) *Mol. Biol. Cell* **4,** 1251–1266
24. van Weert, A. W., Dunn, K. W., Gueze, H. J., Maxfield, F. R., and Stoorvogel, W. (1995) *J. Cell Biol.* **130,** 821–834
25. Seed, B., and Aruffo, A. (1987) *Proc. Natl. Acad. Sci. U. S. A.* **84,** 3365–3369
26. Cole, N. B., and Lippincott-Schwartz, J. (1995) *Curr. Opin. Cell. Biol.* **7,** 55–64
27. Kelly, R. B. (1990) *Cell* **61,** 5–7
28. Fuchs, R., Schmid, S., and Mellman, I. (1989) *Proc. Natl. Acad. Sci. U. S. A.* **86,** 539–543
29. Presley, J. F., Mayor, S., McGraw, T. E., Dunn, K. W., and Maxfield, F. R. (1997) *J. Biol. Chem.* **272,** 13929–13936
30. Fuchs, R., Male, P., and Mellman, I. (1989) *J. Biol. Chem.* **264,** 2212–2220
31. Lukacs, G. L., Rotstein, O. D., and Grinstein, S. (1991) *J. Biol. Chem.* **266,** 24540–24548
32. Kim, J. H., Lingwood, C. A., Williams, D. B., Furuya, W., Manolson, M. F., and Grinstein, S. (1996) *J. Cell Biol.* **134,** 1387–1399
33. Demaurex, N., Furuya, W., D'Souza, S., Bonifacino, J. S., and Grinstein, S. (1998) *J. Biol. Chem.* **273,** 2044–2051
34. Mayor, S., Presley, J. F., and Maxfield, F. R. (1993) *J. Cell Biol.* **121,** 1257–1269
35. D'Souza, S., Garcia-Cabado, A., Yu, F., Teter, K., Lukacs, G., Skorecki, K., Moore, H.-P., Orlowski, J., and Grinstein, S. (1998) *J. Biol. Chem.* **273,** 2035–2043
36. Rybak, S., Lanni, F., and Murphy, R. (1997) *Biophys. J.* **73,** 674–87
37. Orci, L., Halban, P., Perrelet, A., Amherdt, M., Ravazzola, M., and Anderson, R. G. (1994) *J. Cell Biol.* **126,** 1149–1156
38. Link, E., McMahon, H., Fischer von Mollard, G., Yamasaki, S., Niemann, H., Sudhof, T. C., and Jahn, R. (1993) *J. Biol. Chem.* **268,** 18423–18426
39. Bennett, M. K. (1995) *Curr. Opin. Cell Biol.* **7,** 581–586
40. Johnson, A. O., Ghosh, R. N., Dunn, K. W., Garippa, R., Park, J., Mayor, S., Maxfield, F. R., and McGraw, T. E. (1996) *J. Cell Biol.* **135,** 1749–1762